

#### Contents lists available at ScienceDirect

# Fuel

journal homepage: www.elsevier.com/locate/fuel



#### Review article

# Perspective on the role of particle size measurements in gas hydrate agglomeration predictions

Hannah M. Stoner, Carolyn A. Koh

Center for Hydrate Research, Colorado School of Mines - Department of Chemical and Biological Engineering, 1613 Illinois Street, Golden, CO 80401, USA



#### ARTICLE INFO

Keywords:
Gas hydrate
Agglomeration
Particle size distribution
Flow assurance
Viscosity model

#### ABSTRACT

Particle agglomeration plays a major role in the mechanism of gas hydrate accumulation and pipeline plugging. Gas hydrates are solid inclusion compounds composed of natural gas trapped in a three-dimensional water lattice that can form in petroleum flow lines and impede fluid transfer. Agglomeration mechanics are complex yet essential to creating reliable and accurate rheological models for optimizing fluid flow operations, of which the state-of-the-art includes the contact-induced and shear-induced agglomeration models. Particle size distribution measurements of water droplets in an oil-continuous phase reacting to form gas hydrate agglomerates over time can be performed using *in situ* focused beam reflectance measurement (FBRM) and particle video microscope (PVM) probes, or other similar tools. Particle sizing and interfacial interaction measurements form the basis of gas hydrate hydrodynamic multiphase flow models, which incorporate particle agglomeration/viscosity models and the capillary bridge theory-based cohesion model. *In situ* particle sizing probes can also serve as a supplementary process indicator of gas hydrate formation onset. It is essential to perform *in situ* particle-scale experiments to develop and validate an accurate gas hydrate agglomeration model, which is integral to state-of-the-art hydrate flow assurance modeling and risk assessment.

# 1. Brief history and introduction

Agglomeration is the process of particles in a system coming together to form a larger structure through various binding mechanisms, in particular solid-water or solid-solid interactions. It is a common phenomenon in many fields and studied widely. Understanding agglomeration also requires information on particle size distribution and interfacial interactions and how they can change within a system over time. Applications include colloids [1], water ice crystallization in refrigerants [2], or condition alteration in food and drink processing to change characteristics including density or dispersibility [3]. The field of gas hydrates requires knowledge of both agglomeration and particle size distribution when investigating hydrate formation and deposition in petroleum pipelines. The following review presents the key mechanistic pathways to hydrate agglomeration, the evolution of particle size analysis experiments, and the development of particle agglomeration models that are critical to hydrate management strategies (Fig. 1).

Gas hydrates are a type of inclusion compound which, since the 18th

century, were viewed as laboratory curiosities and not considered to have any practical applications. Inclusion compounds, termed clathrates by H.M. Powell, are a class of chemical compounds that involve the "complete enclosure of a molecule by one or more molecules in such a way that it cannot escape from its position [4]." The description of clathrates emerged in scientific works as early as 1811 [5] and continued to appear occasionally through the mid-20th century to present day [6]. One specific type of clathrate compound is called a natural gas hydrate (further referred to as hydrates). These are composed of water molecules trapping natural gas within a cage-like structure (Fig. 2). Gas hydrate studies increased sharply after their industrial discovery by Hammerschmidt in 1934 [7]. During a plant inspection, solid ice-like compounds were found blocking a natural gas pipeline posing production delays. This paper sparked industry-wide interest and began the modern research era of gas hydrates [8].

Although naturally occurring hydrate deposits have also been discovered in permafrost and marine environments [9,10], this paper will focus on the applications of flow assurance within petroleum

Abbreviations: AA, anti-agglomerant; CLD, chord length distribution; C&P, Camargo and Palermo; DEM, discrete element method; DLS, dynamic light scattering; FBRM, focused beam reflectance measurement; KHI, kinetic hydrate inhibitor; LDHI, low dosage hydrate inhibitor; O/W, oil-in-water; PBM, population balance model; PCS, photon correlation spectroscopy; PVM, particle video microscope; THI, thermodynamic hydrate inhibitor; W/O, water-in-oil.

E-mail address: ckoh@mines.edu (C.A. Koh).

<sup>\*</sup> Corresponding author.

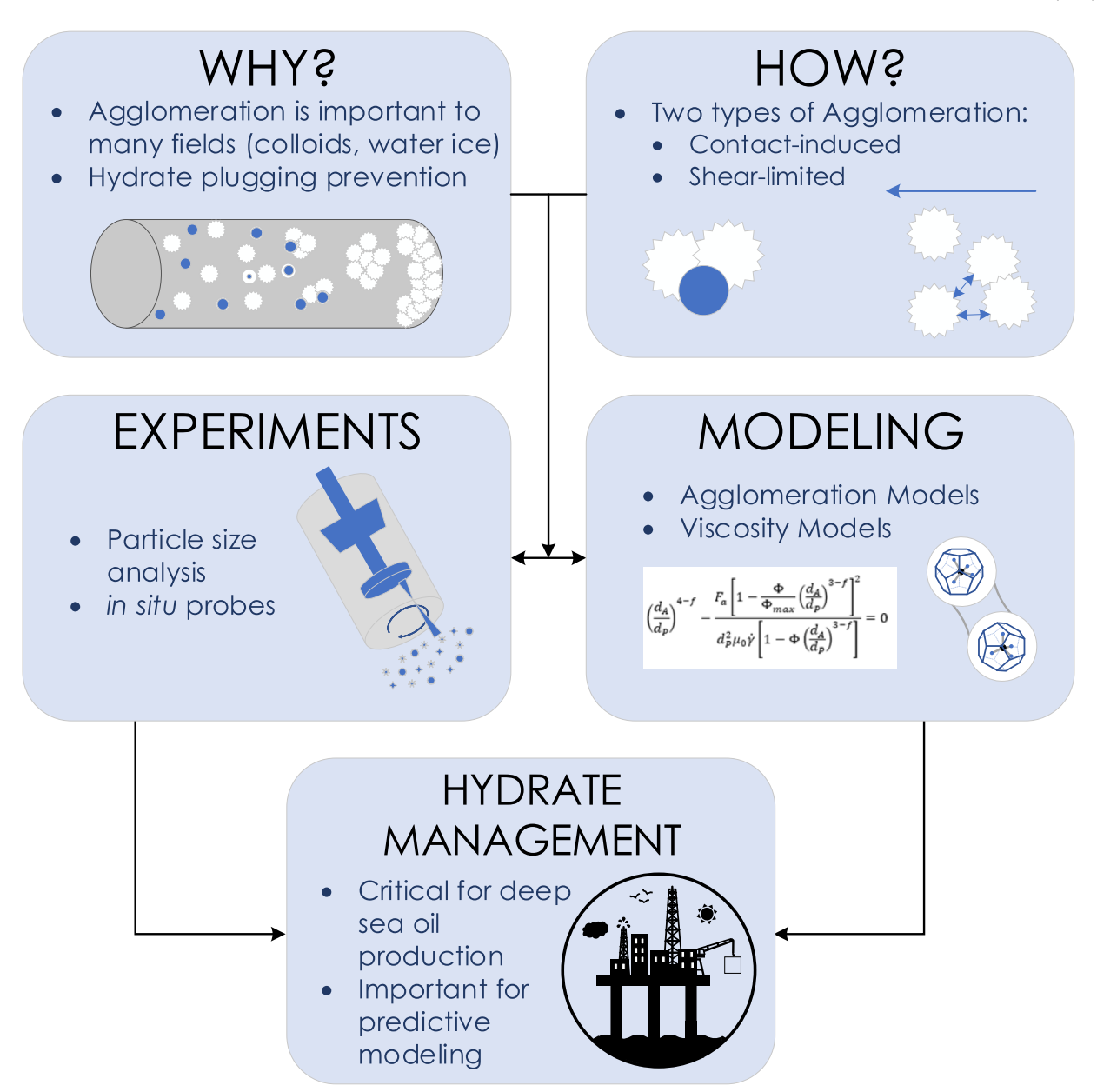
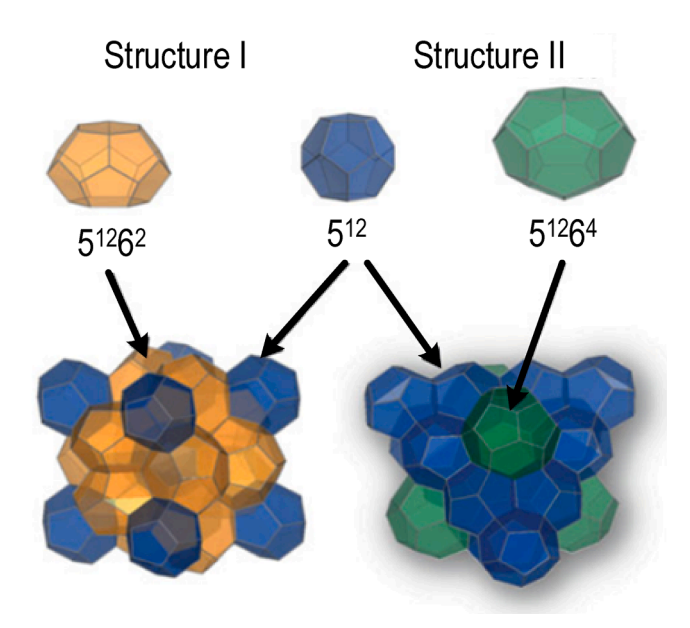


Fig. 1. Schematic of the role of particle size and interfacial interactions on gas hydrate agglomeration and plugging of petroleum pipelines: Agglomeration plays an important role in gas hydrates and other fields including colloids and studies of water ice. Understanding agglomeration is key for hydrate plugging prevention. In situ probes for particle size analysis and agglomeration coupled with viscosity models are critical for deep sea oil production and the development of predictive hydrate models.

pipelines. Flow assurance is the mitigation of solid deposits within pipelines, including asphaltenes [11], waxes [12], scale [13], and hydrates [8]. Hydrates can form when water and gas come into contact, with or without mixing, under high pressure and low temperature conditions, making subsea pipelines an ideal environment. Due to the transient, short time-scale at which they form, hydrates are considered a major problem in flow assurance [14]. If left untreated, hydrate deposits can increase in size until they completely plug a pipeline. Due to pressure buildup on either side of the plug (or between if there are multiple), handling can be also hazardous. There have been fatalities caused by improper safety precautions taken during dissociation of a plug [8]. Since hydrate deposits may cause significant production loss due to increased back pressure from higher viscosity and thus lower production rates, it is important to understand how they form to minimize their impact.

As the petroleum industry moves away from complete hydrate

avoidance (thermodynamic) strategies towards hydrate management (kinetic) strategies, understanding the formation and agglomeration process plays a critical role [16]. Instead of fully preventing pipelines from entering the hydrate stability zone, there is increasing interest in cautiously running deepwater operations within the hydrate domain. To do this, natural characteristics of the crude oil are utilized and/or commercial chemicals are added to the pipeline to allow flow as a slurry of crude oil and hydrate particle suspensions [17]. These chemicals can include thermodynamic hydrate inhibitors (THIs), like methanol [18], or low dosage hydrate inhibitors (LDHIs), including kinetic hydrate inhibitors (KHIs) or anti-agglomerants (AAs). AAs work by allowing hydrates to form but minimize the extent of capillary bridging and particle/interfacial interaction. Typical AAs have a quaternary ammonium salt structure with a hydrophobic tail and a 'hydrate-philic' head group [19]. Even in small doses (<5 vol%), AAs can effectively turn hydrate particles into dispersions that allow flow as a hydrate



**Fig. 2.** The two most common hydrate crystal structures, structure I and structure II: The  $5^{12}$  cage is a cage with 12 pentagonal faces. The  $5^{12}6^2$  cage has 12 pentagonal faces and 2 hexagonal faces. The  $5^{12}6^4$  cage has 12 pentagonal faces and 4 hexagonal faces. The type of structure formed depends on the guest molecule. Natural hydrate deposits are often structure I, as they contain primarily methane. Hydrates that form in pipelines are normally structure II since they can contain light hydrocarbons including methane, ethane, and propane. (Modified from [15]).

transportable slurry instead of forming a plug. As mitigation strategies are not the primary focus of this paper, a detailed review of LDHIs and other management tactics can be found in the literature [16,20].

Continuing to understand the interfacial activity of hydrates and how they interact and agglomerate is essential to the development of deepwater petroleum production. An important aspect of this understanding is the ability to model and predict hydrate agglomeration behavior in a pipeline. Although hydrate nucleation is stochastic, understanding how the agglomerate size and consequently viscosity and other fluid behaviors change with time and system conditions will help scientists and engineers to optimize operating practices to enhance oil and gas production. In addition, agglomeration/slurry flow can provide valuable insight for other technological applications of hydrates including desalination [21], gas separation [22], and natural gas storage [23].

#### 2. Mechanics of agglomeration

#### 2.1. Role of agglomeration in hydrate plugging of pipelines

Fig. 3 shows a conceptual picture of how hydrates form within a pipeline. Due to the turbulence and mixing that occurs, one phase can become entrained in another forming an emulsion. Emulsions become stabilized by surface active agents, which can occur naturally in the oil, or be added to the system. These surfactants accumulate at the hydrocarbon-water interface of the droplets, lowering the interfacial tension and thereby further promoting the anti-agglomeration process [24]. With conducive temperature and pressure conditions, hydrates stochastically nucleate and porous shells begin to form around the water droplets. Hydrate nucleation is a complicated process and the reader is directed to other sources for more information [25,26]. As the particles/ droplets come into contact with one another, they 'stick' or agglomerate due to cohesive forces and capillary bridging. As these agglomerates become larger, they eventually become too heavy and sink to the bottom of the (oil-dominated) pipeline, also called bedding [27,28]. This hydrate bed becomes larger as more agglomerates descend and/or stick to the pipe. The plug may continue to entrain water and oil and grow until it restricts flow or completely blocks the pipeline.

#### 2.2. Conceptual agglomeration mechanisms

The two main agglomeration mechanisms include the contactinduced agglomeration mechanism [32] and the shear-limited agglomeration mechanism [33] (Fig. 4). Contact-induced agglomeration refers to agglomeration caused by water droplet-hydrate interactions, either from a water droplet converting directly to hydrate, or from a water droplet contacting an already established particle/agglomerate [30]. It has been also suggested that the hydrate particle can create its own water layer through surface melting to decrease the interfacial energy and become more thermodynamically stable [34]. This allows for capillary bridging to occur where hydrate particles that are close enough to minimize their contact with the bulk phase (i.e. hydrocarbon) and decrease their interfacial energy. Once the surface water of one hydrate particle is in contact with the hydrate phase or surface water of the second particle, the attractive force/interaction increases, and it becomes harder to separate the two. The latter is typically observed over time. Then the water bridge can convert to hydrate (sintering) and the size of the agglomerate increases. As the particle size increases in the system, the viscosity also increases, which eventually inhibits hydrocarbon production via increased friction. The interfacial energy can be also affected by surface active agents (both natural and commercially added) and by the shell porosity as core water migration can occur [35]. Shear-limited agglomeration highlights a fractal approach to

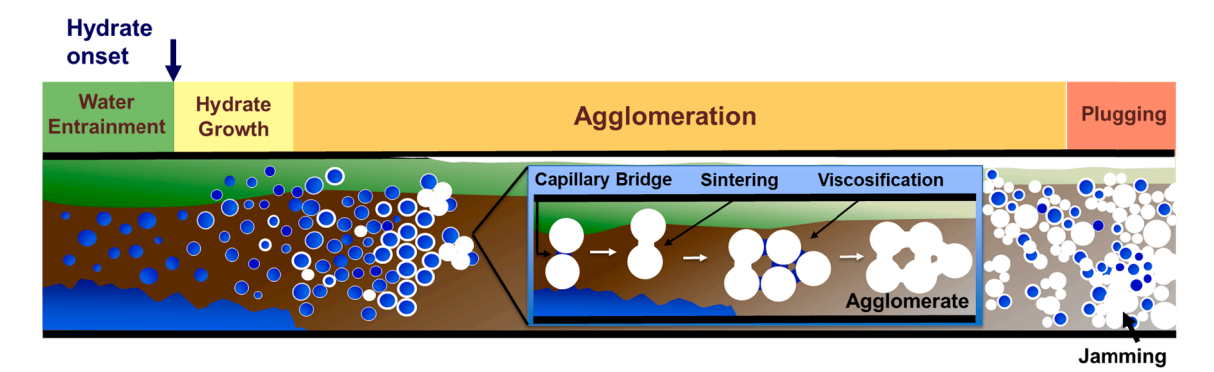


Fig. 3. Schematic diagram of hydrate formation and agglomeration in a pipeline: Water can become entrained in the hydrocarbon phases from the turbulence of the pipeline. Hydrates then nucleate around water droplets to form hydrate shells, which will eventually convert the entire droplet to hydrate. Due to capillary bridging, hydrate particles can stick together and sinter to form larger hydrate agglomerates. This causes viscosification of the pipeline and can eventually lead to jamming and plugging. (Modified from [29–31]).

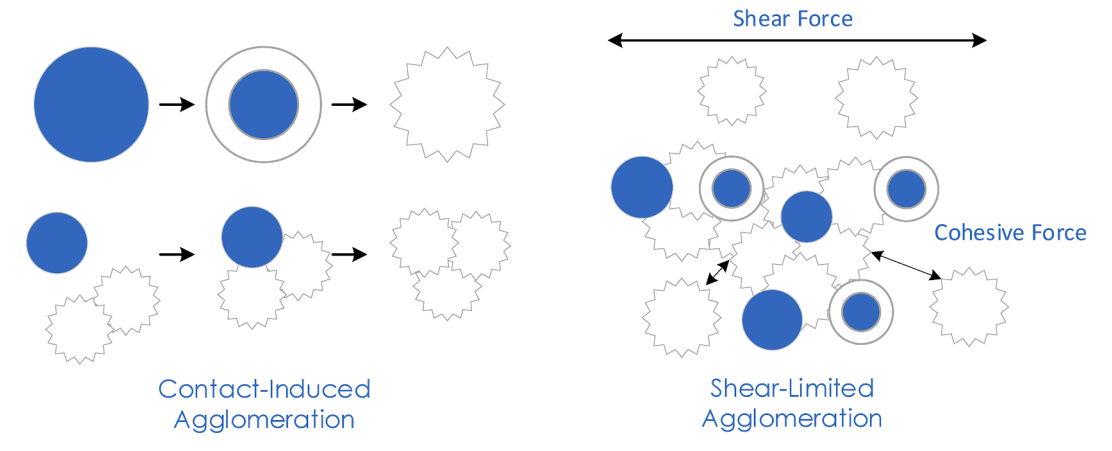
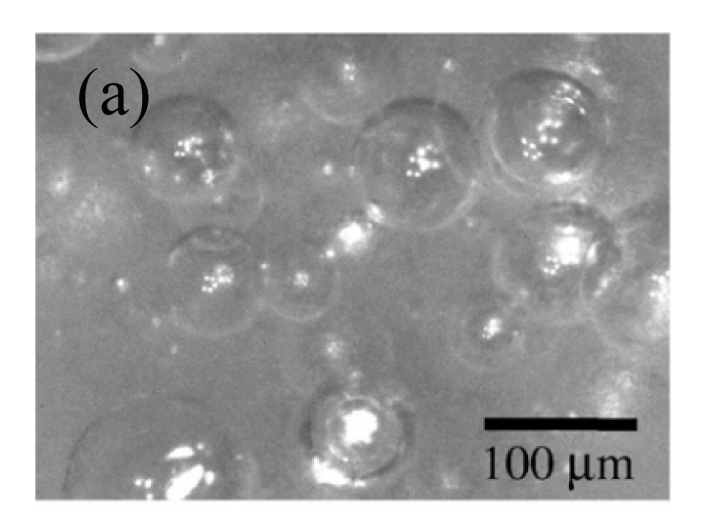
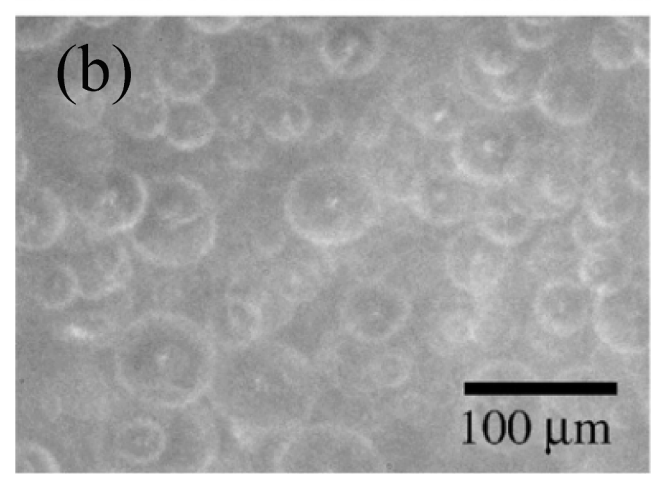


Fig. 4. Schematic diagram of contact-induced and shear-limited agglomeration as described by: Contact induced agglomeration occurs when a water droplet (blue) converts directly to hydrate (white) or when a water droplet comes into contact with an already formed hydrate. Shear-limited agglomeration occurs when adhesive forces between water droplets and hydrate particles is larger than the shear force trying to break them apart [32,33]. (For interpretation of the references to colour in this figure legend, the reader is referred to the web version of this article.)





**Fig. 5.** Experimental images of a water in oil emulsion; (a) emulsified water droplets (b) suspended hydrate particles (from [38]).

determine agglomeration, based on balances between shear force exerted on the hydrates and cohesive forces (via capillary bridging) between hydrate particles through hydrate-hydrate particle interactions as described in the previous paragraph. These mechanisms are illustrated in Fig. 4. This mechanism suggests that once all water droplets suspended in the system have been converted to hydrate, further

agglomeration due to contact with free water droplets will cease. However, experiments show that this is not the case. Colombel et al. recognized that these two models (contact-induced and shear-limited agglomeration) are normally addressed as separate phenomena, but that they should be considered together to fully capture hydrate agglomeration and growth [36]. They suggest relating the two using a population balance model (PBM) where "the agglomeration kernel is related to the contact-induced mechanism and the fragmentation kernel is related to the shear-limited mechanism" [36]. The following section (section 3) discusses experiments related to hydrate agglomeration and particle size analysis. Different modeling and simulation attempts are discussed in more detail in Section 4.

# 3. Droplet and agglomeration sizes determined by experiment

#### 3.1. Why is droplet size important to agglomeration?

Since hydrate deposits and plugs within petroleum pipelines cause major production problems, it is important to understand the key plug formation processes. Currently, hydrate agglomeration is not fully understood. Since hydrate particles can evolve from emulsions, it is essential to understand emulsion size (dispersed droplets in a continuous liquid hydrocarbon phase) and stability as a precursor to agglomeration [37]. The size of the initial water droplet can be directly related to the initial hydrate size in the system, as shown in Fig. 5.

Droplet size also directly effects the rheology of emulsions and eventually the hydrate agglomerate/slurry characteristics. In general, smaller droplets and a narrow size distribution in a water-in-oil (W/O) emulsion will increase the viscosity of the fluid [24]. Smaller droplets are also considered to form more stable emulsions meaning that it is more difficult for them to coalesce [24]. Aside from increased flow resistance, smaller droplets in W/O emulsions also provide a larger surface area of water-hydrocarbon contact. This increased contact facilitates hydrate nucleation as hydrate formation occurs at the water-hydrocarbon interface and full conversion of the water droplets to hydrates. This creates a 'dry hydrate' slurry which is superior for transportation of hydrates [39,40]. Understanding how droplet size changes with system parameters is influential to emulsion size and agglomeration mechanisms of hydrates [41].

# 3.2. Early attempts at particle size analysis

Early attempts at determining particle size within a system came from a model developed by Randolph and Larson [42], also discussed in Section 4. Their work derived equations relating transient population

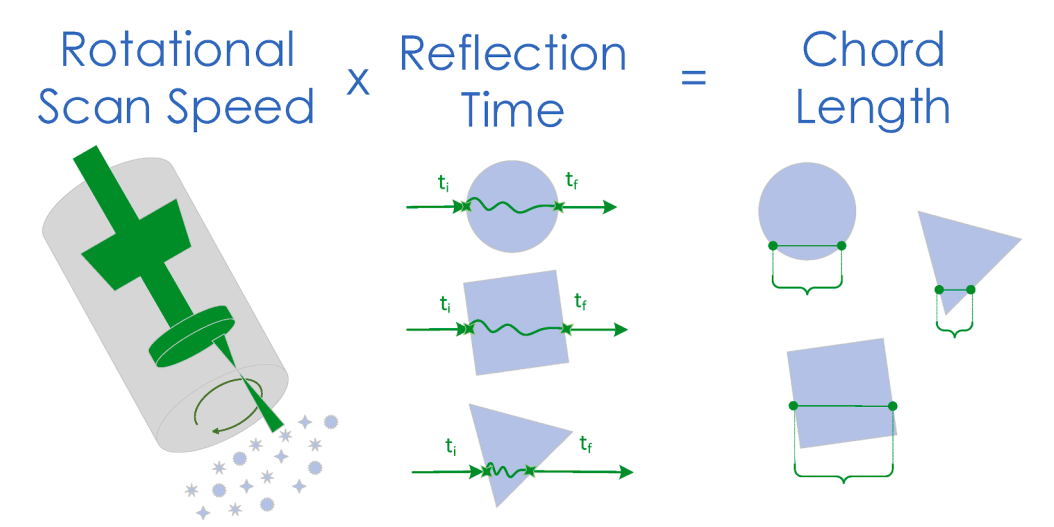


Fig. 6. Schematic of how the FBRM, focused beam reflectance measurement, probe scans a particle to calculate the chord length: with a set rotational scan speed, the probe can calculate different chord lengths by multiplying the scan speed by the time it takes the laser to scan one particle. Modified from [38].

density to size using a general population balance for an arbitrary suspension of particles based on transport properties alone. Although it was more focused on nanoscale particles, it emphasized the need for an experimental method to measure particle size growth rates and system changes in order to refine their model. In 1987, Englezos and Bishnoi et al. created an intrinsic kinetic model for methane hydrates with one adjustable system parameter [43]. The associated experiments measured the gas consumption rate over time with pressure and temperature data to determine the kinetic relationships of hydrate formation. Although their proposed mechanistic model described the data well, the global reaction rate was dependent on the second moment of the particle size distribution of the droplets/agglomerates in the system, which was difficult to actually measure at that time. This, again, stressed the need of an experimental method to determine particle size distributions. Their results were later suggested by Skovborg in 1993 [44] to be overestimated, but it was the first attempt to experimentally determine particle sizes.

Initial work by Nerheim et al. marks early *in situ* experimental attempts at particle sizing. This group utilized Photon Correlation Spectroscopy (PCS, later known as Dynamic Light Scattering, DLS) to study hydrate crystal size and early growth on the nanoscale [45]. Although PCS presented issues with inaccuracy of measurements at low concentrations or due to changes in temperature gradient of the sample volume from hydrate formation, this early work did suggest that *in situ* particle measurements were applicable and possible for hydrate suspension systems.

Unlike Nerheim et al. who measured actual particle size (diameter), Monfort and Nzihou used laser diffraction granulometry on structure I cyclopropane hydrates [46] to measure volume distribution. This made possible the quantification of the second moment of particle size distributions, as previously studied by Englezos and Bishnoi. This also marked a turning point for experiments, as the granulometer was measuring particles in the size range of  $\sim 5$  –  $560 \, \mu m$ , which is on the scale of emulsions and agglomerates instead of hydrate nuclei on a nanoscale. Crawley et al. later performed size analysis of particle suspensions using a turbidometer, which is another in situ laser scattering particle size analysis tool, when looking at the rheology of a granular system [47]. Both the granulometer and turbidity sensor were preferred over other particle sizing techniques because they could be performed in situ, as sampling and ex situ (e.g., microscopy) techniques can alter the state of the system. Crawley et al. showed how it was theoretically possible to calculate the size distribution from the measured turbidity spectrum. This technique was later utilized by Herri et al. to investigate the crystallization mechanism of methane hydrates [48]. Work by this group, again, suggested a relationship between gas consumption and crystal growth rate, as proposed previously by Monfort and Nzihou. Using the turbidity meter, they were able to obtain data in the range of  $10-150~\mu m$  and showed a dependence of mean diameter and number of particles on the stirring rate. Herri et al. continued this work to show the reproducibility of the turbidity meter compared to previous techniques [49].

# 3.3. In situ particle size analysis

With different types of equipment being tested, the 1990's saw the introduction of laser backscattering methods being used to characterize emulsions, which is now one of the more popular techniques for particle size analysis. Sparks and Dobbs were one of the first to characterize an oil-in-water (O/W) emulsion system with this technique [50]. Their results were reproducible and reasonably accurate for highly reflective particles (such as hydrated alumina) but were less accurate for more transparent systems like the O/W emulsion. They also reported poor sensitivity for finer particles ( $< \sim 50 \mu m$ ), which would be addressed later on in the literature [31]. Now, a common and popular laser backscattering technique to determine water droplet size in a water-inoil (W/O) emulsion or hydrate particle/agglomerate size in situ is the Focused Beam Reflectance Measurement (FBRM) probe. An FBRM probe can be used on multiple experimental scales including a benchtop autoclave up to a pilot scale flow loop. The FBRM works by directly inserting the probe into the system at an angle to track particle size distributions using a laser. A laser is transmitted through a set of optic lenses to focus the beam on the sapphire viewing window. The optic lens is then rotated at a precise speed and the laser traces a circle around the window. As the laser beam contacts an individual particle, the light backscatters creating a distinct intensity peak that is recorded by the laser detector. The duration of each intensity peak can be then multiplied by the rotational scanning speed to determine the chord length of the particle The instrument then reports the Chord Length Distributions (CLD) that can be utilized to perform statistical calculations of the droplet or particle/agglomerate size distribution of the system over time. A schematic of this process is shown in Fig. 6. Calibration of this instrument can be conducted by using spherical beads of known size distribution (confirmed by microscopy) to determine the accuracy of the FBRM probe [38].

# 3.4. Limitations of particle sizing measurement methods

It is also important to understand the limitations of the particle sizing

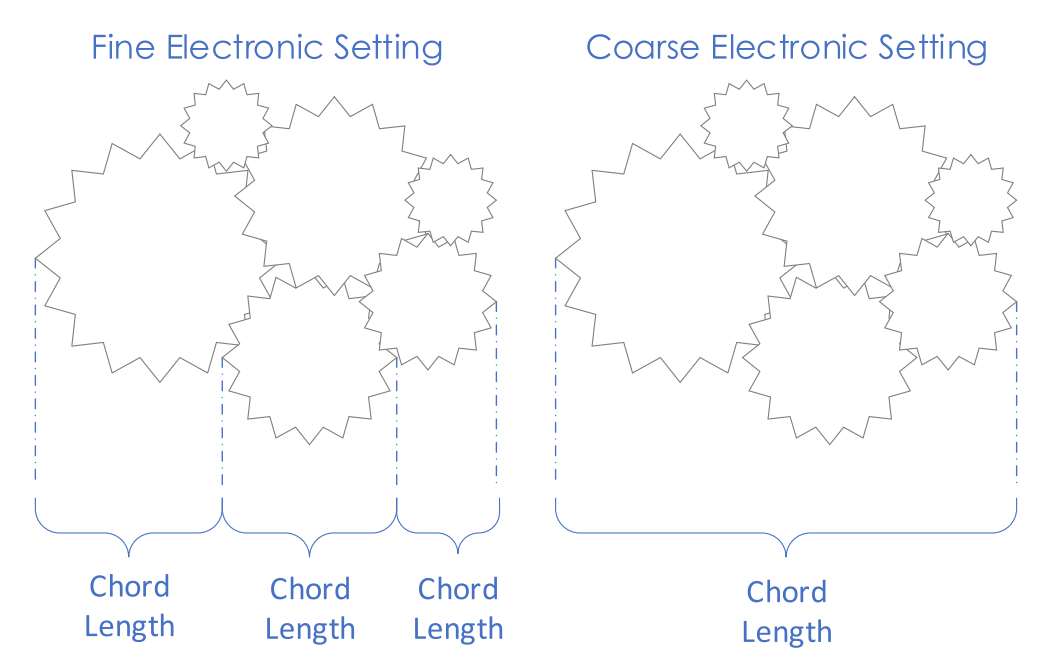


**Fig. 7.** Difference in chord length measurements based on electronic setting: A fine electronic setting can pick up the chord length of individual particles that make up an agglomerate but not the chord length of the entire agglomerate. A coarse electronic setting can pick up the chord length of the entire agglomerate, but not the individual particles of which it is comprised. Modified from [51].

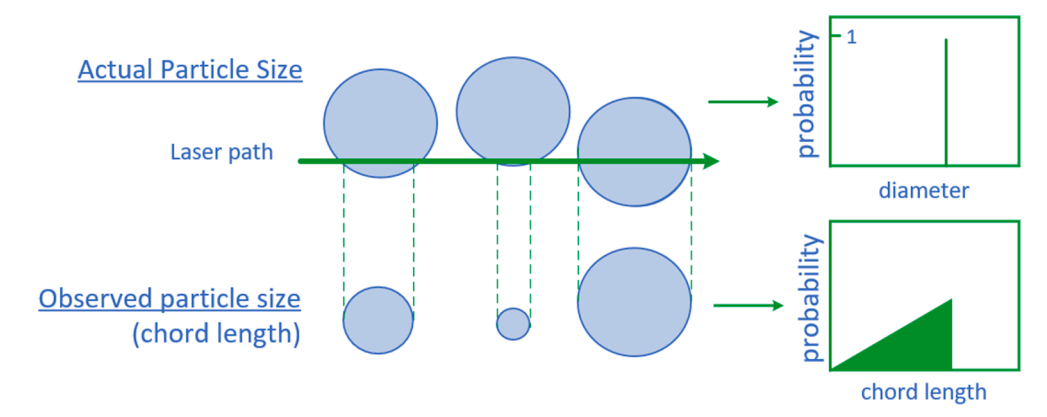


Fig. 8. Effect of particle distance from probe - Depending on the distance the particles are from the probe, different chord lengths will be reported. This example shows how a monodispersed system can have an observed size distribution. Modified from [31].

device. First, it was suggested by Turner [31] that the electronic setting used by the FBRM probe can have an effect on the results. For example, a finer setting can pick up the chord lengths of smaller individual particles, even if they are part of a larger aggregate, as seen in Fig. 7. Fig. 7 also shows the result of using a coarser electronic setting which may result in the probe picking up a single chord length for an aggregate made up of smaller pieces. Turner also mentioned that the reported chord lengths of non-spherical particles may not be completely accurate, as the orientation of the particle at the time of measurement will alter the observed chord length. Turner also mentions that mono-sized particles still produce a size distribution based on their distance from the probe when hit by the laser, as illustrated in Fig. 8.

Due to the restrictions previously mentioned, it is desirable to use an FBRM probe in conjunction with a Particle Video Microscope (PVM) probe (discussed in this work), or a Canty Probe. These can be installed adjacent to an FBRM probe to provide visual evidence of what is being recorded. This acts as an additional check to corroborate what the FBRM probe is recording and visualizes what is happening within the system. A PVM also provides dimensioning and aspect ratio data so that manual measurements can be taken to verify FBRM data. A PVM is also useful in

helping to calibrate the FBRM probe. Unfortunately, it is possible for hydrates to deposit onto the viewing windows of both FBRM and PVM probes. If deposition occurs, the size distribution data collected will not be accurate for the remainder of the experiment. Coating strategies have been developed [51] to hinder the process, but deposition may still occur. It is important when utilizing PVM and/or FBRM probe data to confirm whether or not deposition happens during an experiment, and to fully understand what is occurring within the system. Comparisons of other conventional sizing techniques (e.g., scanning electron microscopy (SEM), DLS, optical microscopy, etc.) to FBRM have been performed to show comparable measurements. For a detailed description the reader is directed to the work of Heath et al. [52] and Li et al. [53].

# 3.5. Recent experiments and the state-of-the-art of in situ particle size analysis

The use of *in situ* particle size analyzers (FBRM and/or PVM) has become common practice over the past two decades for experiments investigating droplet size/emulsion stability, hydrate particle and agglomerate size, and the study of hydrate slurry flow. Even with its

limitations, it can still be used with relative ease at different scales from benchtop autoclaves to flow loops. Use of FBRM is especially helpful at larger flowloop scales because it can still give an indication of what is happening at the micron (particle) scale. The FBRM (and others such as SOPAT, Insitec, or Parsum probes) has become a versatile tool used in numerous experiments. Some examples are described below. It should also be noted that water droplet conversion to hydrate cannot be detected until their size exceeds 1  $\mu$ m in diameter [54].

Similar to early experiments, Clark and Bishnoi expanded the model used by Englezos and Bishnoi et al. in 1987 to determine the intrinsic kinetics of a carbon dioxide hydrate in a semi batch reactor [55]. The FBRM was used to measure CLD to determine the sampling volume needed to calculate the moments of distribution. This approach was applied to a mixture of gases, carbon dioxide and methane hydrate [56]. The FBRM and PVM were also used in an autoclave by Greaves et al. in 2008 to show how the dissociation of agglomerates can change the emulsion type (O/W to W/O) at high water cuts [54]. Boxall et al. were able to continue this work to show that the CLD for W/O emulsions of different oils of varying viscosity and shear rates are usually log-normal distributions from both autoclave and flowloop tests [57]. Herri et al. used the FBRM in a flow loop as a technique to help indicate the hydrate induction time [58]. A sharp increase in the mean chord length accompanied a system pressure drop to indicate hydrate formation. The increase in CLD can be attributed to hydrate particles becoming larger and also beginning to agglomerate. This behavior has also been noted in other studies on methane hydrates in an autoclave using FBRM and PVM [59,60].

Although the FBRM has been mainly used to understand the effects of system parameters, such as water cut and additive dosage of AAs [61,62], on the general slurry flow of hydrates, recent experiments have highlighted other applications of FBRM and PVM. For example, Salmin et al. utilized the PVM to characterize the performance of AAs [63]. By monitoring the CLD over the course of the experiment, it was determined to what extent the AA was affecting agglomeration by determining changes in the CLD and mean chord length. FBRM and PVM probes have been also utilized to assess the amount of methane micro bubbles before hydrate formation and during hydrate reformation to confirm evidence of a memory effect [64,65].

## 4. Agglomeration modeling

#### 4.1. Particle agglomeration and suspension viscosity models

Since a water/hydrocarbon system can evolve from emulsified droplets to small hydrate crystals/particles to larger hydrate agglomerates, the rheology of the system can change dramatically with time. It is critical to understand and model the rheology of hydrate systems correctly to improve the accuracy of hydrate formation and plugging predictions in pipelines. Changes in system viscosity can be a key indicator of plug formation. One of the most well-known rheological models for hydrates is the Camargo and Palermo (C&P) model [66]. This model relates suspension viscosity to aggregate size with the following equation (Eq. (1)).

$$\left(\frac{d_A}{d_P}\right)^{4-f} - \frac{F_a \left[1 - \frac{\Phi}{\Phi_{max}} \left(\frac{d_A}{d_P}\right)^{3-f}\right]^2}{d_P^2 \mu_0 \dot{\gamma} \left[1 - \Phi\left(\frac{d_A}{d_P}\right)^{3-f}\right]} = 0$$
(1)

Here,  $d_A$  is the aggregate diameter,  $d_P$  is the individual particle diameter,  $F_a$  is the cohesion force between particles,  $\Phi$  is the particle volume fraction,  $\Phi_{max}$  is the maximum theoretical particle fraction (4/7 for spheres),  $\mu_0$  is the viscosity of the dispersing liquid,  $\gamma$  is the shear rate, and f is the fractal dimension. Known or measurable quantities include:  $F_a$  which can be measured with a micro-mechanical force apparatus

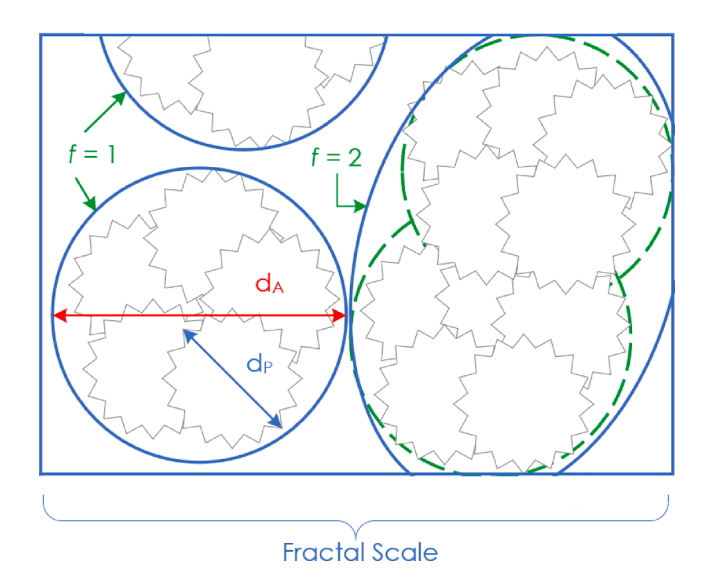


**Fig. 9.** Illustration of  $d_P$ ,  $d_A$ , and f:  $d_P$  represents the diameter of the hydrate particle.  $d_A$  represents the diameter of the hydrate aggregate, which contains individual hydrate particles. f represents the fractal dimension which is the degree of repetition of a given shape on the fractal scale. Modified from [33].

[67],  $\dot{\gamma}$  is a controlled system parameter,  $\Phi$  can be chosen or measured based on estimated particle packing,  $\Phi_{max}$  is a known quantity based on (assumed) geometry, and  $\mu_0$  is a known quantity based on the dispersant (i.e. oil). Originally,  $d_p$  was measured from a system sample using optical microscopy assuming that the hydrate particles were spherical and had identical diameters to the water droplets in the system [66].  $d_A$  is considered  $d_{A,\max}$  at equilibrium, which can also be modeled with the following equation (Eq. (2)), proposed by Mühle [68].

$$d_{A,max} \approx \left[ \frac{F_a(d_p)^{2-f}}{\mu_0 \dot{\gamma}} \right]^{\frac{1}{4-f}} \tag{2}$$

With the introduction of FBRM/PVM probes for image analysis, the values for  $d_A$  and  $d_P$  can be measured *in situ* as well. The fractal dimension, f, was chosen to be 2.5 based on aggregates under shear conditions reported by Hoekstra et al. [69]. The differences in  $d_A$ ,  $d_P$  and f can be seen in Fig. 9.

Camargo and Palermo calculated the relative viscosity ( $\mu_r$ ) of the system (ratio of suspension viscosity to dispersant viscosity) with an equation proposed by Mills [70] (Eq. (3)). Due to the fractal structure, it was also proposed that an effective particle volume fraction should be used instead (Eq. (4)) [70]. Colombel et al. used another equation to calculated the final aggregate size by relating it to the shear stress of the system (Eq. (5)) [36]. Here,  $\tau_0$  is the critical shear stress where aggregates can no longer form, and m is an exponent value based on the breakage mechanism. (Again,  $\Phi$  is the particle volume fraction,  $\Phi_{eff}$  is the effective particle volume fraction,  $\Phi_{max}$  is the maximum theoretical particle fraction (4/7 for spheres), and  $\mu$  is the viscosity of the suspension).

$$\mu_r = \frac{1 - \Phi}{\left(1 - \frac{\Phi}{\Phi_{max}}\right)^2} \tag{3}$$

$$\Phi_{eff} pprox \Phi \left(rac{d_A}{d_P}
ight)^{3-f}$$
 (4)

$$d_A = d_P \left(\frac{\tau_0}{\tau}\right)^m \tag{5}$$

Experiments were performed in both a flow loop and rheological cell. By setting different values of  $\Phi$ , data of shear rate versus relative

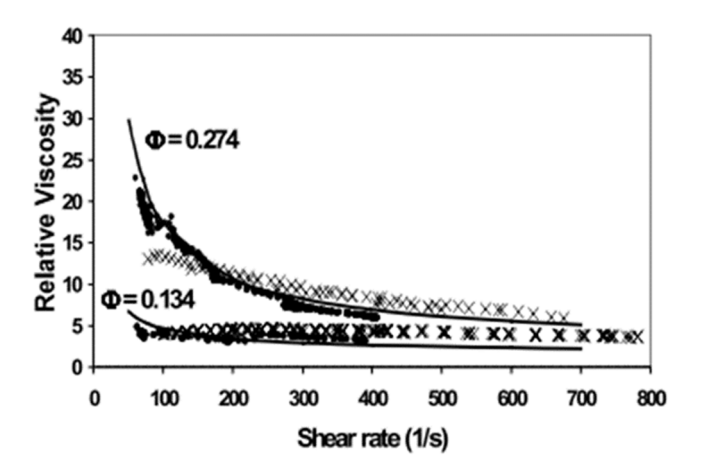


**Fig. 10.** Shear vs. viscosity: This plot shows a comparison of the C&P model (solid lines) at two different hydrate volume fractions with data from a flow loop (dots) and a reaction cell (x's). The model represents the data relatively well and shows that increasing the volume fraction of hydrate increases the relative viscosity of the system. From [66].

viscosity could be fit using the C&P and Mills models, as shown in Fig. 10.

With continued advances in particle size analysis (e.g., from FBRM/PVM), it has become easier to measure certain parameters, including  $d_A$ 

and  $d_P$ , possible to measure  $\Phi$  based on gas consumption data, and the fractal dimension, f. With better estimates for these parameters, the viscosity of a hydrate slurry system can be more accurately modeled. The sensitivity of the C&P model and the Mills model to selected system parameters (aggregate diameter,  $d_A$ , and cohesion force,  $F_a$ ) can be seen in Fig. 11. Fig. 11a shows the relationship between  $F_a$  and  $d_A$  at varying  $d_P$  and shows that increasing  $F_a$  will give larger aggregates and the effect is more prominent at larger values of  $d_P$ . Fig. 11b shows the relationship between  $\Phi_{eff}$  and  $\mu_r$  at varying d<sub>P</sub>, and shows that increasing  $\Phi_{eff}$  will increase  $\mu_P$ , regardless of  $d_P$ . Fig. 11c shows that increasing the value of  $d_A$  gives an increased  $\mu_r$ , but the effect is larger at smaller values of  $d_P$  (at fixed  $\Phi$ ). These three relationships are intuitive based on experimental observations, e.g., [37]. However, the non-intuitive trend shown in Fig. 11d should be noted. This plot shows that increasing  $\Phi$  gives a smaller  $d_A$  at a constant  $d_P$  This indicates that with more particles in the system,  $d_A$  should be smaller even though more hydrates are available to form more aggregates. It is hypothesized that this could be due to increased shear from having more particles in the system. Further studies to examine this relationship more closely are ongoing.

Aside from the relative viscosity of the system, other important rheological properties, such as the yield stress, can be also highly dependent on the particle size. Higher yield stresses indicate the need for a higher shear stress to break apart hydrate aggregates. In turn, hydrate slurries with higher yield stresses will be more likely to plug. Although not discussed in detail here, previous studies have shown the rheologic behavior, including the yield stress, is highly dependent on the water

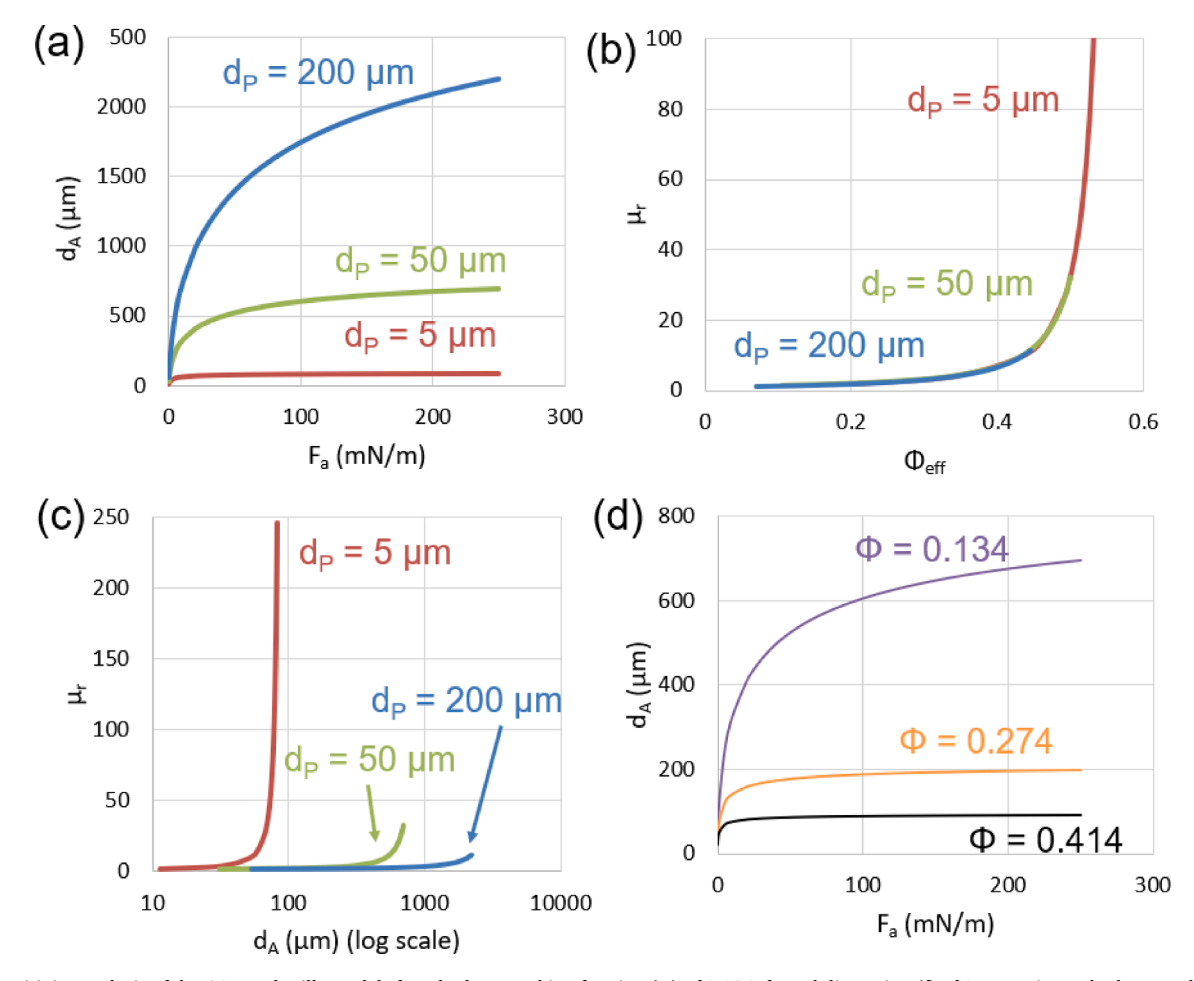
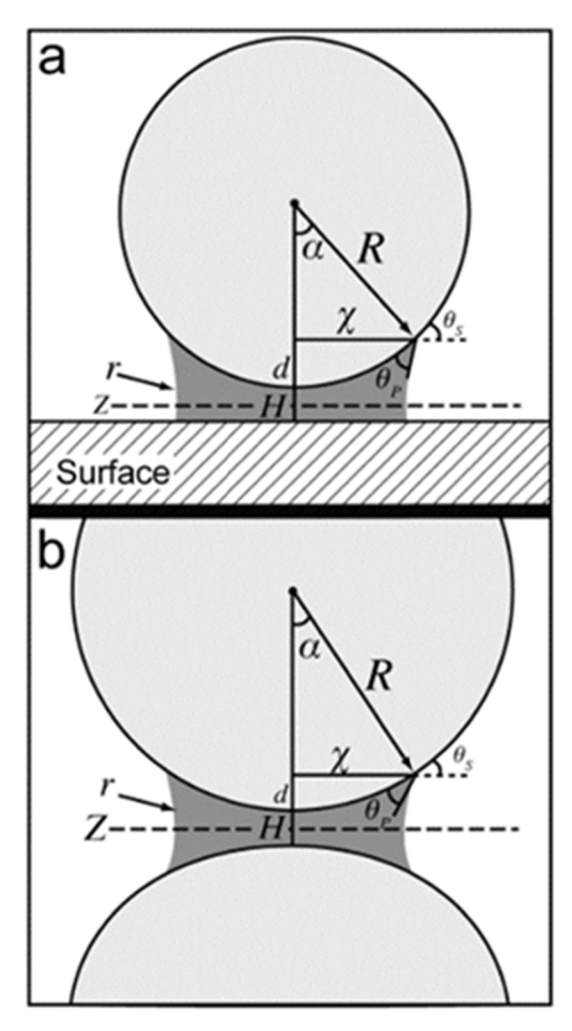


Fig. 11. Sensitivity analysis of the C&P and Mills models for a hydrate packing fraction (Φ) of 0.134, fractal dimension (f) of 2.5, maximum hydrate packing fraction ( $\Phi_{max}$ ) of 0.571, dispersing liquid viscosity ( $\mu_0$ ) of 60 cP, and a shear rate (γ) of 50 s<sup>-1</sup>. (a) effect of force ( $F_a$ ) on aggregate diameter ( $d_A$ ), (b) effect of the effective hydrate packing fraction ( $\Phi_{eff}$ ) on the relative viscosity ( $\mu_r$ ), (c) effect of aggregate diameter ( $d_A$ ) on the relative viscosity ( $\mu_r$ ). (d) effect of force ( $F_a$ ) on aggregate diameter ( $d_A$ ) for varying packing fractions ( $\Phi$ ) and a particle diameter ( $d_p$ ) of 50 μm.



**Fig. 12.** Capillary bridging of (a) particle and surface, (b) particle and particle. Here R is the particle radius, r is the radius of curvature of the liquid bridge,  $\alpha$  is the embracing angle,  $\chi$  is the capillary bridge width,  $\theta_S$  is the external contact angle,  $\theta_P$  is the contact angle, d is the liquid bridge immersion depth, H is the liquid bridge height, and Z is the symmetry plane of the liquid bridge. From [34].

volume fraction of the system. The water fraction can affect the hydrate conversion and number of aggregates formed. Larger aggregates may require different levels of shear to prevent jamming or plugging [71–76]. This behavior has been shown for ice/crude oil systems [71], cyclopentane hydrate systems [72,73], and gas hydrate systems [74,75].

Fig. 11 demonstrates the important role that particle size and agglomerate size play in effecting viscosity and ultimately hydrate plugging potential.

# 4.2. Capillary bridge theory

While the C&P model describes the changes in viscosity of the system at the bulk-scale, the Capillary Bridge Theory can provide some insights into how agglomeration is occurring between individual hydrate particles. As briefly mentioned in section 2.1, capillary attraction forces play a major role in hydrate agglomeration. Since free water droplets emulsified in the system are more attracted to the hydrate particles than the bulk hydrocarbon (Figs. 3 and 4), they will try to maximize their surface area in contact with the hydrate phase to minimize interfacial energy. Water can also come from surface melting and core water migration. If water is coating or partially coating the outside of a hydrate particle and another passes close by, the water may attract the other particle creating a capillary bridge. This can also occur between a hydrate particle and a

surface, such as the pipe wall, as shown in Fig. 12.

In Fig. 12,  $\alpha$  is the embracing angle, R is the particle radius,  $\chi$  is the liquid bridge length,  $\theta_P$  is the contact angle,  $\theta_S$  is the external contact angle, d is the liquid bridge immersion depth calculated by Eqs. (7) (Eq. (7)), H is the particle separation distance, r is the bridge radius of curvature, and Z is the liquid bridge symmetry plane. The capillary force, or the force required to deform this bridge is of the following form (Eq. (6)) and is derived from the free energy equation for the liquid bridge. For an in-depth discussion and derivation of this equation, the reader is directed to the literature [34,77].

$$\frac{F}{R^*} = \frac{2\pi\gamma\cos\theta_P}{1 + \frac{H}{2d}} + 2\pi\gamma\sin(\alpha)\sin(\theta_P + \alpha)$$
 (6)

$$d = \frac{H}{2} \left( -1 + \sqrt{1 + \frac{2(\pi R^{*2} \alpha^2 H + 0.5\pi R^{*3} \alpha^4)}{\pi R H^2}} \right)$$
 (7)

Here,  $\gamma$  is the interfacial tension and  $R^*$  is the normalized particle radius shown in equation (8).  $R_1$  and  $R_2$  represent the radii of the two hydrate particles coming into contact.

$$R^{*} = 2\frac{R_1 R_2}{R_1 + R_2} \tag{8}$$

The capillary bridge thickness (*H*) displayed in Fig. 12 could be potentially measured with atomic force microscopy of a hydrate/water system (similar to that performed for ice by Doppenschmidt [78]), or the force can be measured directly using a Micro-Mechanical Force apparatus [79].

## 4.3. Modeling and simulation studies

Modeling and simulation of hydrate agglomeration is very important. Even with the abundance of experimental data available, more is needed to create transient agglomeration models. Many of the models to be discussed utilize some form of the Mühle Model, C&P Model, Mills Model and/or the Capillary Bridging Model. These models also include the use of a PBM. As briefly mentioned in section 3.2, PBMs use the method of moments to describe population density of suspended particle system properties. PBMs have an advanced derivation and have been described elsewhere [42,80], and will not be discussed further here. As mentioned in Section 2.2, a more comprehensive agglomeration model is needed to accurately model a hydrate system [36], which takes into account particle–particle and particle-droplet interactions for both steady state and especially transient systems.

One of the most comprehensive and applied models of hydrate prediction tools is the Colorado School of Mines Hydrate Kinetics model (CSMHyK). This model utilizes the previously discussed equations including the Mills Model, the C&P Model, and the Capillary Bridging Model [81]. It was initially only designed for oil-dominated systems, using either a kinetic model [82] or a transport model [83], but has since been updated for both water-dominated systems [84] and gas dominated systems [85-87]. Yan et al. brough these models together via an inversion term for when the system switches between a waterdominated and a hydrocarbon-dominated system [88]. CSMHyK has been validated with industrial scale flowloops and field data. CSMHyK is coupled to the transient multiphase flow simulator, OLGATM [89]. The current version of CSMHyK has a Kinetics model and a Transport model. The kinetics model assumes fully dispersed, fixed diameter water droplets suspended in the system, whose hydrocarbon/water contact area is calculated using the Hinze Correlation [90] or the Boxall correlation. Hydrate growth is calculated using modified kinetic equations from Bishnoi et al. [91] and Englezos et al. [43] developed by Boxall et al. [92]. The CSMHyK Transport model makes similar assumptions but models the transport resistances instead of using fitted parameters. As development of CSMHyK has been performed for over a decade, a detailed description will not be discussed and can be found in the

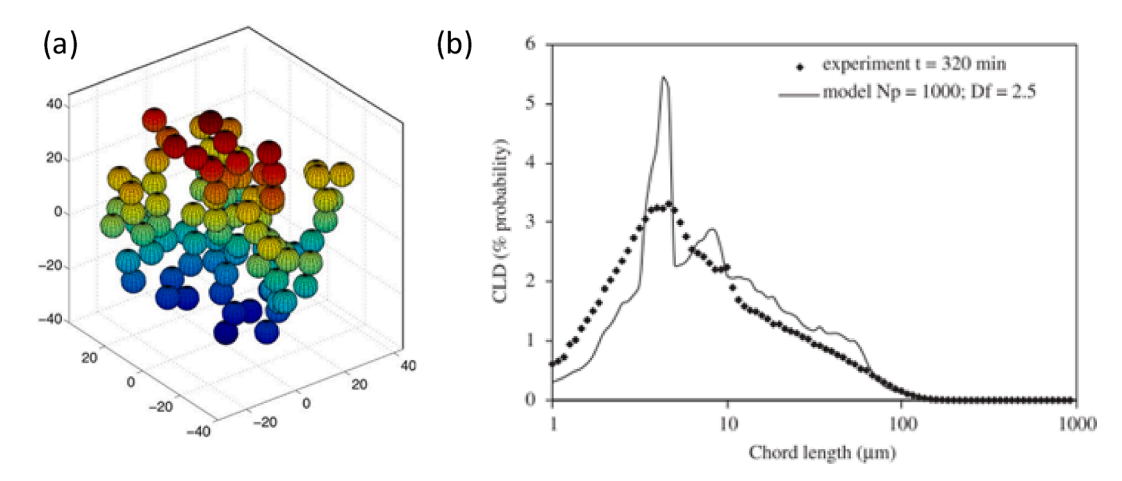


Fig. 13. Example of 3D fractal aggregates modeled by Le Ba et al. (a) This shows an example of 100 spheres generated by a cluster–cluster aggregation model (f = 2.2, N = 100,  $d_P = 5 \mu m$ ); (b) This plot shows an example of the experimental flow loop data (dots) compared to the model (f = 2.5, N = 1000,  $d_P = 4 \mu m$ ). It can be seen that the model gives the same general shape as the experimental data, but it overestimates the maximum probability chord length. From [100].

literature [87,93,94]. CSMHyK continues to be improved to provide a comprehensive model for multiphase fluid systems in different pipeline conditions [95].

Balakin et al. proposed a coupled Eulerian-Eulerian CFD-PBM model confirmed by experimental data that could help improve CSMHyK [96]. Other models have utilized computational fluid dynamics (CFD) with different techniques to model hydrate suspension/slurry systems [97,98]. CFD is a type of numerical analysis to study different fluid mechanics problems. Other modeling methods include CFD coupled with discrete element method (3D DEM), as performed by Rensing et al., to understand the effects agglomeration had on hydrate suspensions [99]. These simulations showed an important perspective that agglomerate shape may be changing even if other aspects, such as fractal dimension, are not. Leba et al. used a different approach by building monodispersed 3D fractal aggregates to simulate their CLD measurements based on FBRM-flow loop data (Fig. 13) [100]. The data suggest that a polydisperse population could give more accurate results.

There have also been suggested updates to the Capillary Bridging Model by Liu et al. to take into account volume changes to the liquid bridge. The proposal included a modified pendular liquid bridge since the conversion of the bridge will reduce the liquid volume and therefore affect other variables and the presented cohesive force, which was confirmed with MMF measurements [101]. There have also been new models suggested for agglomeration between hydrate particles and surfaces, moving away from a hard-sphere model. Developments suggest the adoption of a soft-sphere model due to surface melting and the growth of a quasi-liquid layer [102].

One of the key factors for the development and implementation of a model is its confirmation with experimental data. Although experiments and modeling are often discussed separately, it is imperative these are closely coupled in order to validate and refine the models to create better predictive and reliable simulations.

# 5. Summary and future directions

Hydrate agglomeration is a critical, but not well understood step in pipeline plug formation. As oil and gas production continues to move towards harsher conditions and deeper environments and cost-savings are needed, it is imperative to have accurate and reliable hydrate plugging models for risk assessment. This review provides interconnecting mechanistic and mathematical models, with different experimental and modeling techniques. This included a brief historical overview of particle size analysis and its importance to accurately model hydrate agglomeration. State-of-the-art particle size analysis includes the use of *in situ* FBRM and PVM probes, or other similar technology.

Common models such as the Mühle Model, the Camargo and Palermo Model and the Capillary Bridging Model are discussed, which are integral to hydrate prediction models like CSMHyK. Although experiments and modeling were mostly discussed separately, they are interdependent tools

The measurement of system parameters that affect hydrate agglomeration are key to validate and refine proposed models and mechanisms. In particular, particle sizing, fractal dimension, and inter-particle force have been shown to significantly affect agglomeration, but the interpretation of their measurement outputs can be difficult. With more effort towards their analysis, more accurate agglomeration models can be developed. Another missing key aspect is the existence of a transient agglomeration and rheological model. The models discussed here are applicable to steady state operations and may provide some insight to transient systems, but it is crucial to create a time-dependent model as hydrates are of more concern during transient operations (i.e., shut-ins and restarts). These breakthroughs can lead to more accurate models and will improve hydrate agglomeration predictions for better flow assurance operations/risk assessment.

# **Declaration of Competing Interest**

The authors declare that they have no known competing financial interests or personal relationships that could have appeared to influence the work reported in this paper.

# Acknowledgments

This work was supported financially by the National Science Foundation (CBET Award #2015201).

# References

- Israelachvili JN. Intermolecular and Surface Forces. 3rd ed. Waltham, MA: Elsevier; 2011. https://doi.org/10.1016/B978-0-12-391927-4.10025-8.
- [2] Kasza K, Hayashi K. Ice slurry cooling research: storage tank ice agglomeration and extraction. Am Soc Heating, Refrig Air Cond Eng Conf, Chicago 1999:16.
- [3] Dhanalakshmi K, Ghosal S, Bhattacharya S. Agglomeration of food powder and applications. Crit Rev Food Sci Nutr 2011;51(5):432–41. https://doi.org/ 10.1080/10408391003646270.
- [4] Powell HM. 15. The structure of molecular compounds. Part IV. clathrate compounds. J Chem Soc 1948:61. https://doi.org/10.1039/jr9480000061.
- [5] Sir Humphry Davy. On a combination of oxymuriatic gas and oxygene gas. R Soc Publ 1811;101:155–62.
- [6] Dyadin YA, Terekhova IS, Rodionova TV, Soldatov DV. Half-century history of clathrate chemistry. J Struct Chem 1999;40(5):645–53. https://doi.org/10.1007/ BF02903441.
- [7] Hammerschmidt EG. Formation of gas hydrates in natural gas transmission lines. Ind Eng Chem 1934;26(8):851–5. https://doi.org/10.1021/ie50296a010.

- [8] Sloan ED, Koh CA. Clathrate Hydrates of Natural Gases. 3rd ed. Boca Raton, FL: CRC Press; 2008. https://doi.org/10.1155/2010/706872.
- Makogon Y. Features of natural gas fields exploitation in permafrost zone. Gazov Promyshlennost 1966.
- [10] Collett T, Lewis K, Zyrianova M, Haines S, Schenk C, Mercier T, et al. Assessment of Undiscovered Gas Hydrate Resources in the North Slope of Alaska, 2018. USGS 2019:2016-9. https://doi.org/10.3133.
- [11] Mullins OC. The asphaltenes. Annu Rev Anal Chem 2011;4(1):393-418. https:// oi.org/10.1146/annurev-anchem-061010-113849
- [12] Aiyejina A, Chakrabarti DP, Pilgrim A, Sastry MKS. Wax formation in oil pipelines: A critical review. Int J Multiph Flow 2011;37(7):671-94. https://doi. org/10.1016/j.ijmultiphaseflow.2011.02.007.
- Frenier WW, Formation ZM, Removal,. and Inhibition of Inorganic Scale in the Oilfield Environment. 1st ed. Society of Petroleum Engineers; 2008
- Koh CA, Sloan ED, Sum AK, Wu DT. Fundamentals and Applications of Gas Hydrates. Annu Rev Chem Biomol Eng 2011;2(1):237-57. https://doi.org/ 0.1146/annurev-chembioeng-061010-114152
- [15] Krishna L, Koh CA. Inorganic and methane clathrates: Versatility of guest-host compounds for energy harvesting. MRS Energy Sustain 2015;2:1-17. https://doi. org/10.1557/mre.2015.9
- Kinnari K, Hundseid J, Li X, Askvik KM. Hydrate Management in Practice. J Chem Eng Data 2015;60(2):437-46. https://doi.org/10.1021/je500783u.
- Salmin DC, Delgado-Linares J, Wu DT, Zerpa LE, Koh CA. Hydrate agglomeration in crude oil systems in which the asphaltene aggregation state is artificially modified. Proc Annu Offshore Technol Conf 2019;2019-May. https://doi.org/ 10.4043/29484-ms
- Notz PK. Discussion of the Paper "The Study of Separation of Nitrogen from Methane by Hydrate Formation Using a Novel Apparatus". Ann N Y Acad Sci 1994;715(1 Natural Gas H):425-9. https://doi.org/10.1111/nyas.1994.715. issue-110.1111/j.1749-6632.1994.tb38855.x.
- [19] Perrin A, Musa OM, Steed JW. The chemistry of low dosage clathrate hydrate inhibitors. Chem Soc Rev 2013;42:1996-2015. https://doi.org/10.1039
- [20] Kelland MA. Production Chemicals for the Oil and Gas Industry. 2nd ed. Boca Raton, FL: CRC Press; 2014.
- Khan MN, Peters CJ, Koh CA. Desalination using gas hydrates: The role of crystal nucleation, growth and separation. Desalination 2019;468:114049. https://doi. org/10.1016/j.desal.2019.06.015.
- [22] Li Z-Y, Xia Z-M, Li X-S, Chen Z-Y, Cai J, Li G, et al. Hydrate-Based CO2 Capture from Integrated Gasification Combined Cycle Syngas with Tetra-nbutylammonium Bromide and Nano-Al2O3. Energy Fuels 2018;32(2):2064-72. https://doi.org/10.1021/acs.energyfuels.7b03605.
- Kezirian M, Phoenix S. Natural gas hydrate as a storage mechanism for safe, sustainable and economical production from offshore petroleum reserves. Energies 2017;10(6):828. https://doi.org/10.3390/en10060828. Kokal S, Aramco S. Crude oil emulsions: A state-of-the-art review. San Antonio:
- Soc. Pet. Eng; 2002.
- [25] Khurana M, Yin Z, Linga P. A review of clathrate hydrate nucleation. ACS Sustain Chem Eng 2017;5(12):11176-203. https://doi.org/10.1021/ cssuschemeng 7b03238
- Warrier P. Khan MN. Srivastava V. Maupin CM, Koh CA, Nucleation of clathrate hydrates. J Chem Phys 2016;145(21):211705. https://doi.org/10.1063
- [27] Joshi SV, Grasso GA, Lafond PG, Rao I, Webb E, Zerpa LE, et al. Experimental fl owloop investigations of gas hydrate formation in high water cut systems. Chem Eng Sci 2013;97:198-209. https://doi.org/10.1016/j.ces.2013.04.019.
- Hernandez OC. Investigation of Hydrate Slurry Flow in Horizontal Pipelines. The University of Tulsa 2006.
- [29] Qin H, Srivastava V, Wang H, Zerpa LE, Koh CA. Machine learning models to predict gas hydrate plugging risks using flowloop and field data. Proc Annu Offshore Technol Conf 2019;2019-May.
- [30] Hu S, Koh CA. Interfacial properties and mechanisms dominating gas hydrate cohesion and adhesion in liquid and vapor hydrocarbon phases. Langmuir 2017; 33(42):11299-309. https://doi.org/10.1021/acs.langmuir.7b02676.
- Turner DJ. Clathrate Hydrate Formation in Water-in-Oil Dispersions. Colorado School of Mines 2005.
- [32] Palermo T, Fidel-Dufour A, Maurel P, Peytavy JL, Hurtevent C. Model of hydrates agglomeration - Application to hydrates formation in an acidic crude oil. 12th Int Conf Multiph Prod Technol '05 2005:525-40.
- Pauchard V, Darbouret M, Palermo T, Peytavy JL. Gas hydrate slurry flow in a [33] black oil. Prediction of gas hydrate particles agglomeration and linear pressure drop. In: 13th Int Conf Multiph Prod Technol; 2007. p. 343-55.
- [34] Aman ZM, Brown EP, Sloan ED, Sum AK, Koh CA. Interfacial mechanisms governing cyclopentane clathrate hydrate adhesion/cohesion. Phys Chem Chem Phys 2011;13:19796-806. https://doi.org/10.1039/c1cp21907c.
- Davies SR, Sloan ED, Sum AK, Koh CA. In Situ Studies of the Mass Transfer Mechanism across a Methane Hydrate Film Using High-Resolution Confocal Raman Spectroscopy. J Phys Chem C 2010;114(2):1173-80. https://doi.org/ 10.1021/jp909416v
- [36] Colombel E, Gateau P, Barré L, Gruy F, Palermo T. Discussion of Agglomeration Mechanisms between Hydrate Particles in Water in Oil Emulsions. Oil Gas Sci Technol 2009;64(5):629-36. https://doi.org/10.2516/ogst/2009042
- Sjöblom J, Øvrevoll B, Jentoft G, Lesaint C, Palermo T, Sinquin A, et al. Investigation of the hydrate plugging and non-plugging properties of oils. J Dispers Sci Technol 2010;31(8):1100-19. https://doi.org/10.1080/ 01932690903224698

[38] Greaves D, Boxall J, Mulligan J, Montesi A, Creek J, Dendy Sloan E, et al. Measuring the particle size of a known distribution using the focused beam reflectance measurement technique. Chem Eng Sci 2008;63(22):5410-9. https:// doi.org/10.1016/j.ces.2008.07.023

- [39] Gudmundsson JS, Andersson V, Parlaktuna M. Hydrate Concept for Capturing Associated Gas, 1998.
- Høiland S, Askvik KM, Fotland P, Alagic E, Barth T, Fadnes F. Wettability of Freon hydrates in crude oil/brine emulsions. J Colloid Interface Sci 2005;287(1): 217–25. https://doi.org/10.1016/j.jcis.2005.01.080
- [41] Boxall JA, Koh CA, Sloan ED, Sum AK, Wu DT. Droplet size scaling of water-in-oil emulsions under turbulent flow. Langmuir 2012;28(1):104-10. https://doi.org.
- [42] Randolph AD, Larson MA. Transient and steady state size distributions in continuous mixed suspension crystallizers. AIChE J 1962;8(5):639-45. https:// doi.org/10.1002/(ISSN)1547-590510.1002/aic.v8:510.1002/aic.690080515
- Dholabhai PD, Englezos P, Kalogerakis N, Bishnoi PR. Kinetics of Formation of Methane Hydrates and Gas. Chem Eng Sci 1987;42.
- [44] Skovborg P, Ng HJ, Rasmussen P, Mohn U. Measurement of induction times for the formation of methane and ethane gas hydrates. Chem Eng Sci 1993;48(3): 445-53. https://doi.org/10.1016/0009-2509(93)80299-6.
- Nerheim AR, Svartaas TM, Samuelsen EK. Investigation of hydrate kinetics in the nucleation and early growth phase by laser light scattering. Int. Offshore Polar Eng. Conf. 1992;I:620-7.
- Monfort JP, Nzihou A. Light scattering kinetics study of cyclopropane hydrate growth. J Cryst Growth 1993;128(1-4):1182-6.
- Crawley G, Cournil M, Di Benedetto D. Size analysis of fine particle suspensions by spectral turbidimetry: potential and Limits. Powder Technol 1997;91(3):
- [48] Herri JM, Pic JS, Gruy F, Cournil M. Methane hydrate crystallization mechanism from in-situ particle sizing. AIChE J 1999;45(3):590-602. https://doi.org/ 10.1002/(ISSN)1547-590510.1002/aic.v45:310.1002/aic.690450316.
- [49] Herri JM, Gruy F, Pic JS, Cournil M, Cingotti B, Sinquin A. Interest of in situ turbidimetry for the characterization of methane hydrate crystallization: Application to the study of kinetic inhibitors. Chem Eng Sci 1999;54(12): 1849-58. https://doi.org/10.1016/S0009-2509(98)00433-3.
- Sparks RG, Dobbs CL. The Use of Laser Backscatter Instrumentation for the Online Measurement of the Particle Size Distribution of Emulsions. Part Part Syst Charact 1993;10(5):279-89.
- Greaves D. The Effects of Hydrate Formation and Dissociation on High Water Content Emulsions, Colorado School of Mines 2007.
- Heath AR, Fawell PD, Bahri PA, Swift JD. Estimating average particle size by focused beam reflectance measurement (FBRM). Part Part Syst Charact 2002;19: 84-95. https://doi.org/10.1002/1521-4117(200205)19:2<84::AID-PPSC84>3.0.
- [53] Li M, Wilkinson D, Patchigolla K. Comparison of particle size distributions measured using different techniques. Part Sci Technol 2005;23(3):265-84. https://doi.org/10.1080/02726350590955912
- Greaves D, Boxall J, Mulligan J, Sloan ED, Koh CA. Hydrate formation from high water content-crude oil emulsions. Chem Eng Sci 2008;63(18):4570-9. https:// doi.org/10.1016/j.ces.2008.06.025
- Clarke MA, Bishnoi PR. Determination of the intrinsic kinetics of CO2 gas hydrate formation using in situ particle size analysis. Chem Eng Sci 2005;60:695-709. https://doi.org/10.1016/j.ces.2004.08.040.
- [56] Giraldo C, Maini B, Bishnoi R, Clarke M. A simplified approach to modeling the rate of formation of gas hydrates formed from mixtures of gases. Energy Fuels 2013;27(3):1204-11. https://doi.org/10.1021/ef301483h.
- Boxall JA, Koh CA, Sloan ED, Sum AK, Wu DT. Measurement and calibration of droplet size distributions in water-in-Oil emulsions by particle video microscope and a focused beam reflectance method. Ind Eng Chem Res 2010;49(3):1412-8. //doi.org/10.1021/ie901228e
- [58] Ba H Le, Cameirão A, Herri J, Darbouret M, Peytavi J, Glénat P, et al. The use of FBRM probe during hydrate particles agglomeration 2010.
- Chen J, Liu J, Chen G-J, Sun C-Y, Jia M-L, Liu B, et al. Insights into methane hydrate formation, agglomeration, and dissociation in water + diesel oil dispersed system. Energy Convers Manag 2014;86:886-91. https://doi.org/
- Cameirao A, Serris E, Melchuna A, Herri JM, Glenat P. Monitoring gas hydrate formation and transport in a flow loop with acoustic emission. J Nat Gas Sci Eng 2018;55:331-6. https://doi.org/10.1016/j.jngse.2018.04.035.
- Lv XF, Gong J, Li WQ, Shi BH, Yu D, Wu HH. Experimental study on natural-gashydrate-slurry flow. SPE J 2014;19:206-14. https://doi.org/10.2118/158597-
- Lv Y-N, Sun CY, Liu B, Chen G-J, Gong J. A water droplet size distribution dependent modeling of hydrate formation in water/oil emulsions. AIChE J 2017; 63:1010-23. https://doi.org/10.1002/aic.
- Salmin DC, Majid AAA, Wells J, Sloan ED, Estanga D, Kusinski G, et al. Study of anti-Agglomerant low dosage hydrate inhibitor performance. Proc Annu Offshore Technol Conf 2017;3:1695-711. https://doi.org/10.4043/27911-m
- Maeda N. Interfacial nanobubbles and the memory effect of natural gas hydrates. J Phys Chem C 2018;122(21):11399-406. https://doi.org/10.1021
- [65] Chen Y, Gong J, Shi B, Yao H, Liu Y, Fu S, et al. Investigation into methane hydrate reformation in water-dominated bubbly flow. Fuel 2020;263:116691. https://doi.org/10.1016/j.fuel.2019.116691.
- Camargo R, Palermo T. Rheological Properties of Hydrate Suspensions in an Asphaltenic Crude Oil. Proc Fourth Int Conf Gas Hydrates 2002:880-5.

- [67] Brown EP, Koh CA. Micromechanical measurements of the effect of surfactants on cyclopentane hydrate shell properties. Phys Chem Chem Phys 2016;18(1): 594–600. https://doi.org/10.1039/C5CP06071K.
- [68] Muhle K. Floc stability in laminar and turbulent flow. Coagul. Flocculation Theory Appl. (Surfactant Sci. B. 47). 1st ed., New York, NY: CRC Press; 1993, p. 355–90.
- [69] Hoekstra LL, Vreeker R, Agterof WGM. Aggregation of colloidal nickel hydroxycarbonate studied by light scattering. J Colloid Interface Sci 1992;151(1): 17–25. https://doi.org/10.1016/0021-9797(92)90234-D.
- [70] Mills P. Non-Newtonian behaviour of flocculated suspensions. J Phys Lett 1985; 46(7):301–9.
- [71] Rensing PJ, Liberatore MW, Sum AK, Koh CA, Dendy Sloan E. Viscosity and yield stresses of ice slurries formed in water-in-oil emulsions. J Nonnewton Fluid Mech 2011;166(14-15):859–66. https://doi.org/10.1016/j.jnnfm.2011.05.003.
- [72] Zylyftari G, Lee JW, Morris JF. Salt effects on thermodynamic and rheological properties of hydrate forming emulsions. Chem Eng Sci 2013;95:148–60. https://doi.org/10.1016/j.ces.2013.02.056.
- [73] Ahuja A, Zylyftari G, Morris JF. Yield stress measurements of cyclopentane hydrate slurry. J Nonnewton Fluid Mech 2015;220:116–25. https://doi.org/ 10.1016/j.jnnfm.2014.11.007.
- [74] Fidel-Dufour A, Gruy F, Herri J-M. Rheology of methane hydrate slurries during their crystallization in a water in dodecane emulsion under flowing. Chem Eng Sci 2006;61(2):505–15. https://doi.org/10.1016/j.ces.2005.07.001.
- [75] Webb EB, Rensing PJ, Koh CA, Sloan ED, Sum AK, Liberatore MW. High-pressure rheology of hydrate slurries formed from water-in-oil emulsions. Energy Fuels 2012;26(6):3504–9. https://doi.org/10.1021/ef300163y.
- [76] Majid AAA, Wu DT, Koh CA. A Perspective on Rheological Studies of Gas Hydrate Slurry Properties. Engineering 2018;4(3):321–9. https://doi.org/10.1016/j. eng.2018.05.017
- [77] Aman ZM. Interfacial Phenomena of Cyclopentane Hydrate 2012:240.
- [78] Döppenschmidt A, Kappl M, Butt H-Jürgen. Surface properties of ice studied by atomic force microscopy. J Phys Chem B 1998;102(40):7813–9. https://doi.org/ 10.1021/jp981396s.
- [79] Liu C, Li M, Zhang G, Koh CA. Direct measurements of the interactions between clathrate hydrate particles and water droplets. Phys Chem Chem Phys 2015;17 (30):20021–9. https://doi.org/10.1039/C5CP02247A.
- [80] Randolph AD, Larson MA. Theory of Particulate Processes. 1st ed. New York: Academic Press, Inc.; 1971.
- [81] Zerpa LE, Sloan ED, Sum AK, Koh CA. Overview of CSMHyK: A transient hydrate formation model. J Pet Sci Eng 2012;98–99:122–9. https://doi.org/10.1016/j. petrol.2012.08.017.
- [82] Boxall JA. Hydrate Plug Formation from <50% Water Content Water-in-Oil Emulsions. Colorado School of Mines 2009.
- [83] Davies SR. The Role of Transport Resistances in the Formation and Remediation of Hydrate Plugs. Colorado School of Mines 2009.
- [84] Joshi SV. Experimental Investigation and Modeling of Gas Hydrate Formation in High Water Cut Producing Oil Pipelines. Colorado School of Mines 2012.
- [85] Charlton TB, Di Lorenzo M, Zerpa LE, Koh CA, Johns ML, May EF, et al. Simulating Hydrate Growth and Transport Behavior in Gas-Dominant Flow. Energy Fuels 2018;32(2):1012–23. https://doi.org/10.1021/acs. energyfuels.7b02199.

- [86] Nicholas J. Hydrate Deposition in Water Saturated Liquid Condensate Pipelines. Colorado School of Mines 2008.
- [87] Zerpa LE. A practical model to predict gas hydrate formation, dissociation and transportability in oil and gas flowlines. Colorado School of Mines, 2013.
- [88] Wang Y, Koh CA, Dapena JA, Zerpa LE. A transient simulation model to predict hydrate formation rate in both oil- and water-dominated systems in pipelines. J Nat Gas Sci Eng 2018;58:126–34. https://doi.org/10.1016/j.jngse.2018.08.010.
- [89] Turner D, Boxall J, Yang D, Kleehamer C, Koh C, Miller K, et al. Development of a Hydrate Kinetic Model and Its Incorporation Into the OLGA2000® Transient Multi-Phase Flow Simulator. Proc 5th Int Conf Gas Hydrates 2005.
- [90] Hinze JO. Fundamentals of the hydrodynamic mechanism of splitting in dispersion processes. AIChE J 1955;1(3):289–95. https://doi.org/10.1002/(ISSN) 1547-590510.1002/aic.v1:310.1002/aic.690010303.
- [91] Vysniauskas A, Bishnoi PR. A kinetic study of methane hydrate formation. Chem Eng Sci 1983;38(7):1061–72. https://doi.org/10.1016/0009-2509(83)80027-X.
- [92] Boxall J, Davies S, Koh CA, Sloan ED. Predicting when and where hydrate plugs form in oil-dominated flowlines. SPE Proj Facil Constr 2009;4:80–6. https://doi. org/10.2118/129538-PA.
- [93] Wang Y. The development and application of hydrate formation, transportation and bedding models in liquid-dominated systems. Colorado School of Mines 2019. https://doi.org/10.1017/CBO9781107415324.004.
- [94] Qin H, Qu A, Wang Y, Zerpa L, Koh C, Bodnar S, et al. Predicting hydrate plugging risk in oil dominated systems using atransient hydrate film growth prediction tool. Proc. Annu. Offshore Technol. Conf., vol. 2020- May, Houston, TX: 2020.
- [95] Wang Y, Koh CA, White J, Patel Z, Zerpa LE. Hydrate formation management simulations with anti-agglomerants and thermodynamic inhibitors in a subsea tieback. Fuel 2019;252:458–68. https://doi.org/10.1016/j.fuel.2019.04.146.
- [96] Balakin BV, Lo S, Kosinski P, Hoffmann AC. Modelling agglomeration and deposition of gas hydrates in industrial pipelines with combined CFD-PBM technique. Chem Eng Sci 2016;153:45–57. https://doi.org/10.1016/j. ces.2016.07.010.
- [97] Jassim E, Abdi MA, Muzychka Y. A CFD-based model to locate flow restriction induced hydrate deposition in pipelines. Offshore Technol Conf Proc 2008;1: 213–29
- [98] Lo S. CFD modelling of hydrate formation in oil-dominated flows. Offshore Technol. Conf. 2011;2–5. https://doi.org/10.4043/21509-ms.
- [99] Rensing PJ, Koh CA, Sloan ED, Mustoe GGW. Simulation of hydrate aggregate structure via the discrete element method. 6th Int. Conf. Gas Hydrates, Vancouver: 2008, p. 1–4.
- [100] Leba H, Cameirao A, Herri J-M, Darbouret M, Peytavy J-L, Glénat P. Chord length distributions measurements during crystallization and agglomeration of gas hydrate in a water-in-oil emulsion: Simulation and experimentation. Chem Eng Sci 2010;65(3):1185–200. https://doi.org/10.1016/j.ces.2009.09.074
- [101] Liu C, Li Y, Wang W, Dong S, Li M. Modeling the micromechanical interactions between clathrate hydrate particles and water droplets with reducing liquid volume. Chem Eng Sci 2017;163:44–55. https://doi.org/10.1016/j. ces.2017.01.031.
- [102] Nguyen NN, Berger R, Butt HJ. Premelting-Induced Agglomeration of Hydrates: Theoretical Analysis and Modeling. ACS Appl Mater Interfaces 2020;12(12): 14599–606. https://doi.org/10.1021/acsami.0c0063610.1021/acsami.0c00636.